The Journal of Experimental Biology **199**, 731–740 (1996)
Printed in Great Britain © The Company of Biologists Limited 1996
JEB0245

TARGETTING AND VISUOMOTOR SPACE IN THE LEAF-HOPPER *EMPOASCA VITIS* (GOTHE) (HEMIPTERA: CICADELLIDAE)

JOHN BRACKENBURY

Department of Anatomy, University of Cambridge, Downing Street, Cambridge CB2 3DY, UK

Accepted 16 November 1995

Summary

The accuracy with which the visuomotor system of *Empoasca vitis* can prescribe a jump trajectory towards a bright, uniformly illuminated target shape was investigated. The targets consisted of discs, rings or bars cut out of black card and mounted in front of a source of stroboscopic light diffused through translucent paper. The targets varied in size, subtending angles of 7–110° to the insect's eye. Target resolution was measured independently along the horizontal and vertical axes and was defined in terms of the standard deviation of the horizontal (S.D.*x*) or vertical (S.D.*y*) angular coordinates of the take-off paths measured with respect to the geometric centre of the target. In all cases involving single connected images, the point towards which jumping was directed coincided with the geometric centre of the image area (the light centroid). This meant, for example, that the insects specifically targetted the dark core of a ring of light. No formal features of the target shapes, such as light–dark boundaries, were targetted. Vertical axial resolution was independent of image size (mean S.D.*y* for all image sizes 6.9°), but horizontal axial resolution only achieved this minimal value at intermediate image sizes (approximately 30–60°). When two separate but identical target shapes (vertical bars) were presented at different horizontal separations, the dark area between them was accurately targetted up to target separations of approximately 30–50°. At greater separations, there was an increasing tendency to target one or other of the two shapes. From these experiments it is concluded that, in the frontal visual field, spatial integration can be performed to an accuracy (as defined in these experiments) of 7°×7°. Performance deteriorates outside an optimal range of image sizes, and this is faithfully reflected in the decline in horizontal axial resolution when jumping. However, this decline in visual performance is not reflected in target resolution along the vertical axis because it is masked by a biomechanical constraint, i.e. the inability of the legs to set take-off angles outside a narrow range of 30–60° to the horizontal.

Key words: jump mechanics, visuomotor targetting, visual resolution, biomechanical constraints, leaf-hopper, *Empoasca vitis*.

Introduction

The execution of rapid, precisely targetted visuomotor activities in insects, such as the predatory strikes of mantids, carabid beetles and dragonfly larvae or the predatory darts of adult dragonflies and robber flies (Asilidae), is based on a visual system which is capable of (i) recognising specific target characteristics relating to shape or movement, and (ii) accurately locating the target. Prey image fixation and the saccadic head movements that are associated with it are facilitated by the presence of a fovea in both mantids (Rossel, 1980, 1983) and carabid beetles (Bauer, 1977, 1981). Image characteristics that are known to elicit appetitive behaviour in mantids include size, contrast, direction of movement and orientation (Prete, 1990, 1992, 1993; Prete and Mahaffey, 1993). The latter cues may be based on the presence of specific movement/orientation-sensitive channels, such as those demonstrated in the dragonfly nervous system (Olberg, 1981; O'Carroll, 1993) and which are believed to be involved in image pattern recognition by honeybees (Srinivasan *et al.* 1993; Giger and Srinivasan, 1995).

The visual refinements shown by some predatory insects may be necessary for image recognition, but accurate targetting of an image *per se* can be performed within the framework of a relatively simple visual system. For example, some flea-beetles have a compound eye containing less than 150 ommatidia but can nevertheless jump accurately towards the centre of a brightly lit target (Brackenbury and Wang, 1995). Flea-beetles and other ballistic jumpers provide convenient models for investigating the visual and biomechanical constraints operating on the targetting performance of a simple visuomotor system. The results of the present study show that the visuomotor targetting performance of the leaf-hopper *Empoasca vitis* may be influenced to a differential degree by these constraints depending on target size and shape.

Materials and methods

Kinematic measurements were made on three species of jumping Homoptera caught locally in the field: *Empoasca vitis* (Gothe), *Cercopis vulnerata* (Illiger) and *Philaenus spumarius* (Linnaeus). During experimentation, groups of individuals belonging to a single species were dispensed from a container onto a flat, circular platform measuring 10 cm in diameter and positioned 20–25 cm away from a stroboscopic light source (Drelloscop 1018, Munchengladbach, Germany) (Fig. 1). The stroboscope lamp head was 20 cm in diameter and was covered with several layers of translucent tracing paper in order to diffuse the light uniformly across its face. The light pulse duration and repetition rates were 20 μs and 150 Hz respectively. Once placed on the platform, the insects almost invariably orientated towards the light source, using a smooth turning movement, pivoted on the end of the body and lasting up to 0.5–1 s depending on initial orientation. There was no overshoot of the turning movement, and no obvious signs of peering; the insects either jumped at once or else walked towards the edge of the platform before jumping. Jumping was recorded with the aid of a miniature Panasonic video camera fitted with a 6 mm focal length lens and positioned laterally at right angles to the line connecting the launch platform to the light source (Fig. 1, camera position 1). The camera generated 50 image fields per second, each containing three consecutive images of the leaping insect. Tape-recorded images were analysed frame-by-frame with the aid of a Panasonic AG-7355 video cassette recorder. Take-off angle and take-off velocity in the vertical plane were measured from the initial image trio obtained during take-off. These and subsequent images were also used to calculate body rotation rate and, in two species, the time required to open the wings fully after take-off.

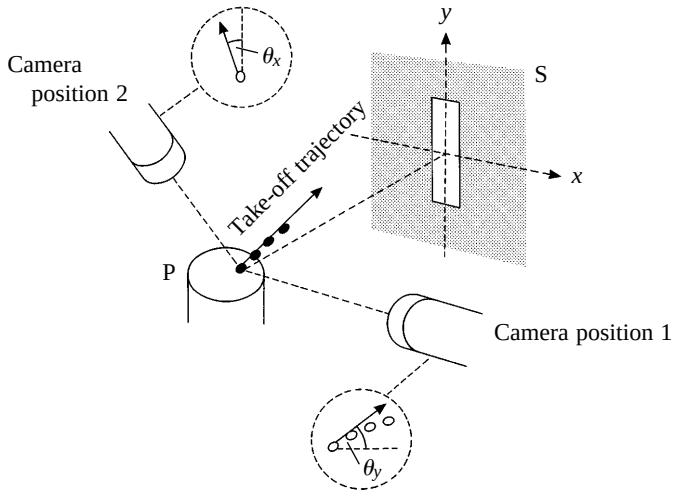

Fig. 1. Method of recording jump kinematics. The insects jumped from a platform P towards a stroboscopic light source S and were recorded by a video camera placed to the side (camera position 1). In the experiments involving *Empoasca vitis*, various shapes were cut out of black card and fixed onto the front of the light source (vertical bar shown). In a separate series of experiments, take-off angles (θ_x and θ_y) were recorded along the vertical (y) or horizontal (x) axes, with respect to the geometric centre of the target shape. In the latter series, two camera positions were used.

A much more exhaustive study, involving an analysis of individual leaps performed by approximately 3000 insects, was undertaken to test the targetting capabilities of *Empoasca vitis*. Insects were collected regularly over a 3 month period from yew trees *Taxus baccata*, and on each occasion they were used within 2 h of capture. The experimental technique was similar to that previously described in a study of flea-beetle jumping (Brackenbury and Wang, 1995). Target shapes were cut out of black card and were mounted directly onto the face of the stroboscope. The black card therefore served as a mask and, since all jumps were performed in dark-room conditions, the insects saw only the brightly illuminated cut-out target image against a black background. Important differences in the targetting behaviour of *Empoasca vitis* when compared with that of the flea-beetle *Aphthona atrocaerulea* had to be taken into account in the experimental design. The latter performs a high-speed, almost linear trajectory towards the target, and the distribution of target 'hits' – the actual impacts upon the target – is a faithful reflection of the coordinates initially set by the insect prior to take-off. In contrast, a simple inspection of the impact points of *Empoasca vitis* upon the surface of the target would suggest that jumping is almost random. It is only by examining the initial trajectory, within the first few centimetres of take-off, that a true measure of the directionality of jumping is obtained. Soon after take-off, once the wings have opened, the initial coordinates appear to be overruled, the motion towards the target becomes more erratic and the insect approaches the target in uncontrolled spirals.

Take-off angles were measured in separate series of experiments either along the vertical axis (camera position 1, Fig. 1) or along the horizontal axis (camera position 2, Fig. 1). In the latter case, in order to reduce any errors arising from parallax, the camera was positioned as accurately as possible at right angles to the take-off path. In all cases, the take-off angles were measured relative to the line projected from the launch point of the insect to the geometrical centre of the target. For analysis, the target area was divided into 10 ° wide zones, along the horizontal and the vertical axes, and target 'hits' were scored in individual zones. This technique produced independent estimates of horizontal and vertical axial target resolution. Axial resolution could then be conveniently quantified in terms of the standard deviation of the scatter of hit-lines about the target centre, either along the vertical axis (S.D.y) or along the horizontal axis (S.D.x). As measured in the present study, the term 'hit' therefore refers not to a physical impact, but to the projection of the take-off trajectory upon the target.

In some instances, the two-dimensional distribution of hits was reconstructed using a graphical technique illustrated in Fig. 2. The advantage of this method of presentation is that it enables another measure of accuracy, 'solid angle' accuracy, to be obtained; the significance of this measure is discussed below. This technique generated a contour map of the hit distribution, each contour line joining points of equal hit

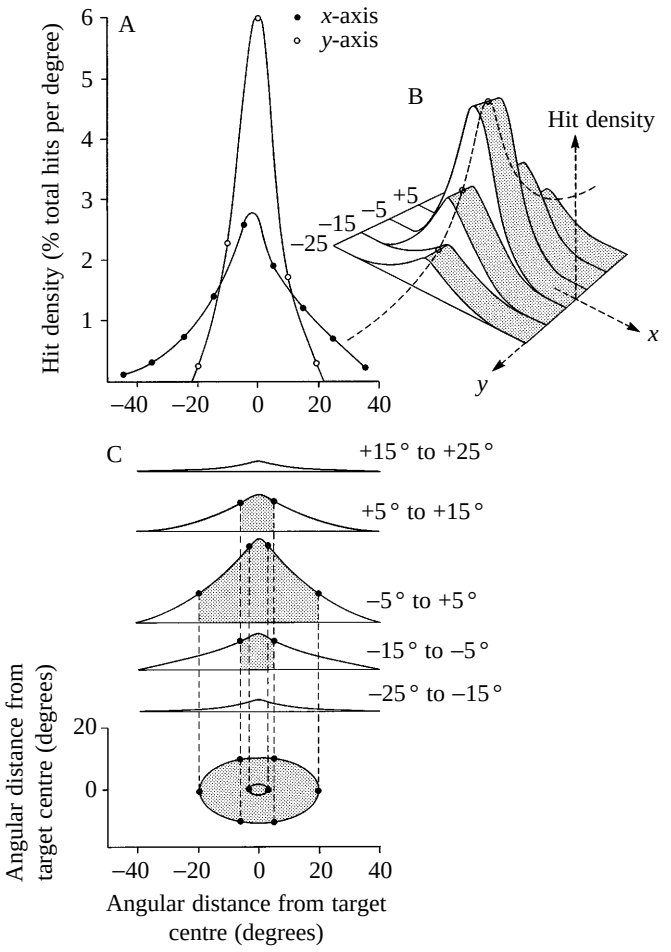

Fig. 2. Method of reconstructing the two-dimensional distribution of take-off trajectories θ_x and θ_y or 'hits' around the target centre. From a notional distribution of θ_x and θ_y given in A, a series of profiles through the two-dimensional hit distribution is reconstructed as in B. The thickness of each profile 'slice' is the same as the data sampling interval i.e. 10°. These profiles are then used to produce the contour map of the trajectories shown in C. Each contour line in C joins points of equal hit density; i.e. trajectories per 10°×10° square of space. Two such contours are represented. The fraction of the total hits lying within the boundaries of individual contours, i.e. between the contour and the target centre, is proportional to the sum of the areas enclosed between the corresponding hit density ordinates on the profiles (shaded areas in C).

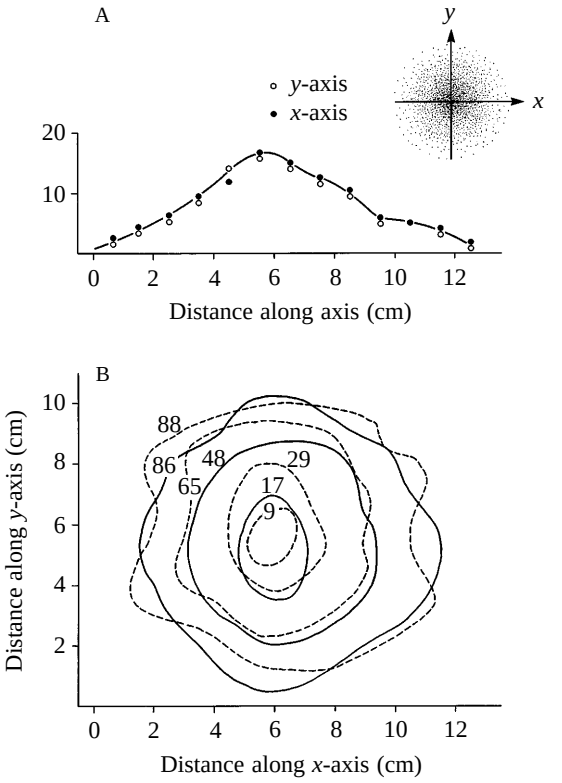

Fig. 3. Reconstruction of a two-dimensional distribution of particles, equivalent to the intersection of a set of hit trajectories with a two-dimensional target. In the first reconstruction, particles were scored on individual 1 cm wide rows (*y*-axis distribution) or columns (*x*-axis distribution), and the results are shown in A. These axial distributions, equivalent to the axial distributions shown in Fig. 2A, were then used to construct a contour map of the particle distribution, shown as the solid lines in B. The second reconstruction, shown by the dashed contour lines in B, was obtained by counting particles on individual squares of the two-dimensional surface. The number superimposed upon each contour line indicates the percentage of total counts located between the contour line and the centre of the distribution.

density, i.e. hits per unit area of target (hits per 10°×10° square of space). In subsequent figures, the number assigned to an individual contour line represents the fraction of all recorded hits that lay within the boundaries of that contour line. The accuracy of this graphical reconstruction technique depends on (i) the thickness of the sample slices made through the target (i.e. 10°, Fig. 2B) and (ii) the assumption that the shape of the target hit distribution, say along the *x*-axis, is the same for all slices. The accuracy of the technique was tested empirically against a two-dimensional radially symmetrical distribution of particles produced by dropping a pinch of salt grains onto a piece of graph paper. Numbers of grains were scored in 1 cm wide slices made parallel to the *y*-axis or the *x*-axis respectively (Fig. 3A), and these data were used to reconstruct the two-dimensional distribution. The contour map generated in this way was compared with that obtained by counting grains on individual square centimetres of 'target' area. Fig. 3C shows that there is a large degree of congruence between the results of the indirect and direct techniques.

Results

The kinematic performance of the three jumping homopterans is shown in Table 1, together with data from three flea-beetles (Brackenbury and Wang, 1995) for comparison. Whilst the take-off velocities of the homopterans occupy a similar range of values to those measured in the different species of flea-beetle, the most notable difference in jumping habit between these two groups is the very slow rotation rates observed in the homopterans.

Table 1. *Kinematics of jumping in Homoptera compared with flea-beetles*

Species	*Empoasca vitis*	*Cercopis vulnerata*	*Philaenus spumarius*	*Aphthona* atrocaerulea*	*Chalcoides* aurata*	*Psylliodes* affinis*
Body length (mm)	4.0±0.1 (8)	9.8±0.1 (10)	6.0±0.2 (7)	1.7±0.1 (6)	2.9±0.1 (5)	2.2±0.1 (6)
Take-off velocity ($m\,s^{-1}$)	1.3±0.1 (25)	2.9±0.1 (16)	4.3±0.7 (29)	1.7±0.3 (31)	0.8±0.1 (9)	2.9±0.1 (49)
Rotation rate (Hz)	5.9±1.6 (26)	5.0±1.0 (10)	9.6±0.3 (27)	66±5 (48)	35±2 (35)	187±11 (9)
Wing opening time (ms)	37±6 (26)	–	60±3 (12)	≈50		

*Flea-beetle data are from Brackenbury and Wang (1995).
Values are means ± S.E.M. (*N*).

Fig. 4 illustrates the targetting performance of *Empoasca vitis* against a bright circular image measuring 7° in diameter and placed at inclinations of 0°, 28° or 56° to the horizontal. The reconstructed two-dimensional hit distributions were essentially the same in all three cases. In particular, the vertical resolution was approximately twice as great as the horizontal resolution (S.D.*y*/S.D.*x* approximately 0.5), resulting in elliptical distributions about the target centre. For a target placed at 0°, the point at which the jump trajectory was aimed lay approximately 30° above the real target centre (Fig. 4A): evidently this target was perceived as accurately as the others, but the insect was incapable of lowering its trajectory to coincide with the horizontal. The lowest practical trajectory when jumping from a horizontal surface appears to be approximately 28–30°. The practical upper limit for take-off angle was investigated by placing the same target directly above the launch platform. Although in this case the insects still attempted to jump towards the target, the mean take-off angle achieved was only 60.5±2.2° (S.E.M., *N*=32). The take-off angles available to *Empoasca vitis* when jumping from a horizontal surface are therefore limited to a quite narrow range of approximately 28–60°. When confronted with a small target located horizontally, *Empoasca vitis* sets its take-off angle at the lowest that is possible biomechanically, and hence overshoots by approximately 30°. The insect can overcome this limitation if given access to a three-dimensional surface with variable inclinations. This flexibility was demonstrated by presenting the insects in a beaker angled towards the target at about 45°. In these circumstances, the majority of the insects delayed their jumping until they had sought out suitable positions on the beaker surface, often jumping either from the sloping lip of the beaker or from an upside-down position on the upper inner side of the beaker. Not surprisingly, the accuracy of jumping from such a complex surface was reduced

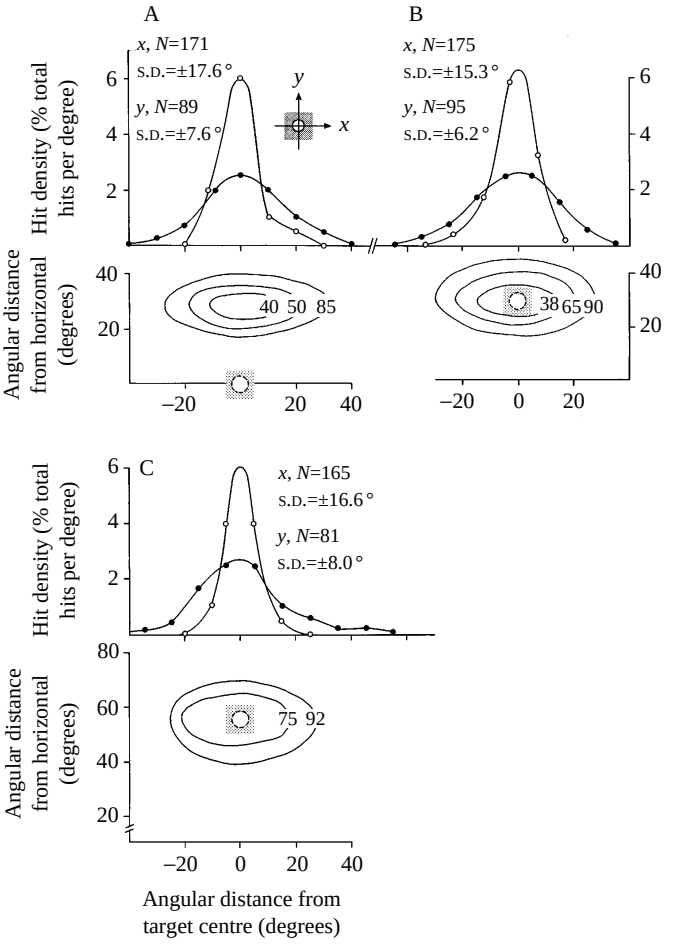

Fig. 4. Jumping performance of *Empoasca vitis* against a 7° diameter disc of light (A, cartoon, inset) located at inclinations of 0°, 28° or 56° (A, B and C respectively) with respect to the launch platform. The upper section of each graph represents the distribution of take-off angles, along the *y*- or *x*-axis, as recorded by camera positions 1 and 2 in Fig. 1, respectively. Zero on the abscissa indicates the centre of the hit distribution. The lower section of each graph shows the reconstructed two-dimensional distribution of trajectories or target 'hits'. The dashed circle represents the correct postion of the target disc on a black background represented by stippling. Only the dark area immediately around the disc is indicated. The number of observations (*N*) and standard deviation (S.D.) for each axial distribution are given. Open circles, θ_y, filled circles, θ_x (see Fig. 2).

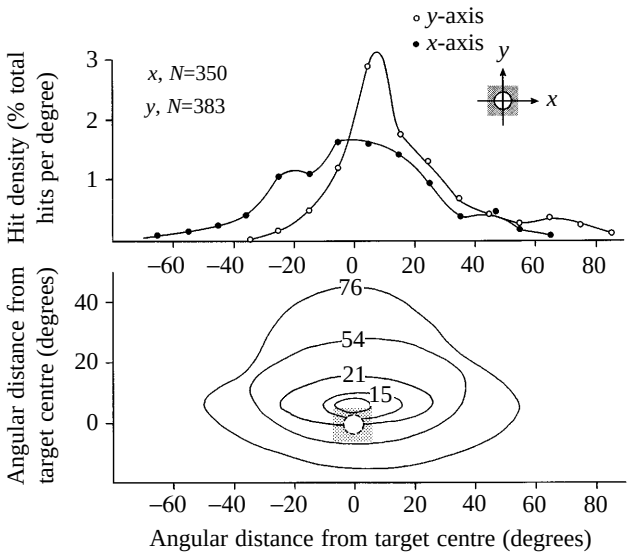

Fig. 5. Jump performance of *Empoasca vitis* leaping from a container tilted towards, and with its mouth directly opposite, a 7° diameter light disc. Other details as in Fig. 4.

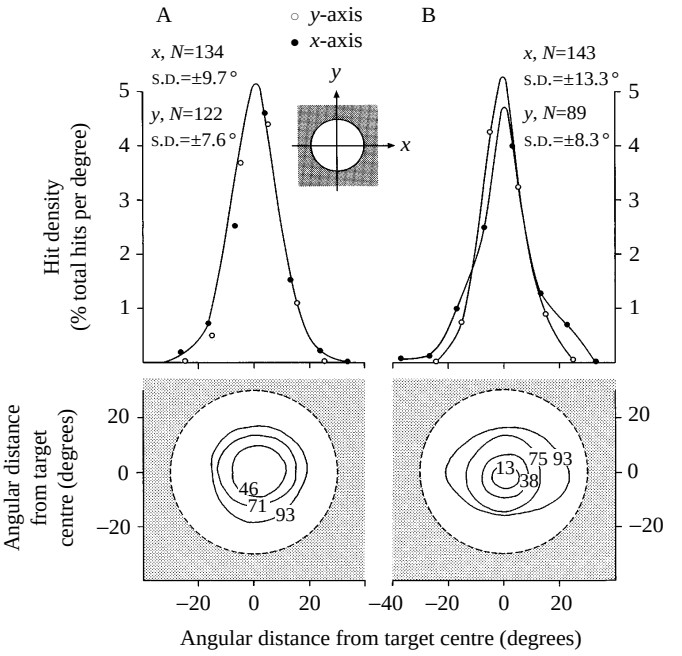

Fig. 6. Jump performance of *Empoasca vitis* against a 60° diameter light disc located at inclinations of 28° (A) or 45° (B) with respect to the launch platform. Other details as in Fig. 4.

but, as Fig. 5 shows, the point at which the jump trajectory was aimed coincided much more closely with the real target centre than when jumping from horizontal ground.

The results of jumping towards a much larger disc, subtending 60° to the insect's eye and centred at inclinations of either 28° or 45°, are shown in Fig. 6. Compared with results for the 7° diameter disc, the hit distributions were much more radially symmetrical, entirely as a result of an increase in horizontal axial resolution. Even so, the horizontal resolution against the 45° target was appreciably worse than against the 28° target. Virtually no hits were scored against the high-contrast boundary of this target, and it was clear that the insects were aiming specifically at the geometric centre of the target.

The above results suggest (i) that a large target is more accurately resolved than a small target; (ii) that the increased accuracy is due to a change in horizontal but not vertical axial resolution; and (iii) that vertical resolution is insensitive to target height, as indicated by the similarity between the S.D.*y* values for the 7° (Fig. 4) and 60° (Fig. 6) targets. The insect also aims specifically at the centroid of the illuminated area and not towards any formal feature such as the boundary. To test the latter hypothesis further, the horizontal axial resolution was measured against a 60° disc containing a 7° black hole located either centrally or eccentrically (Fig. 7A,B). In each case, jumping was targetted at the geometric centre: a 7° black hole inside an illuminated disc, unlike a 7° illuminated disc against a black background (Fig. 4), is not perceived as a target in itself. Approximately 50% of all jumps towards a 60° illuminated disc fall within the central solid angle of 20° (Fig. 6). If the central 20° of such a disc is removed, producing a ring with a dark core, targetting is unaffected (Fig. 7C): the insect continues to locate the centroid of the light pattern,

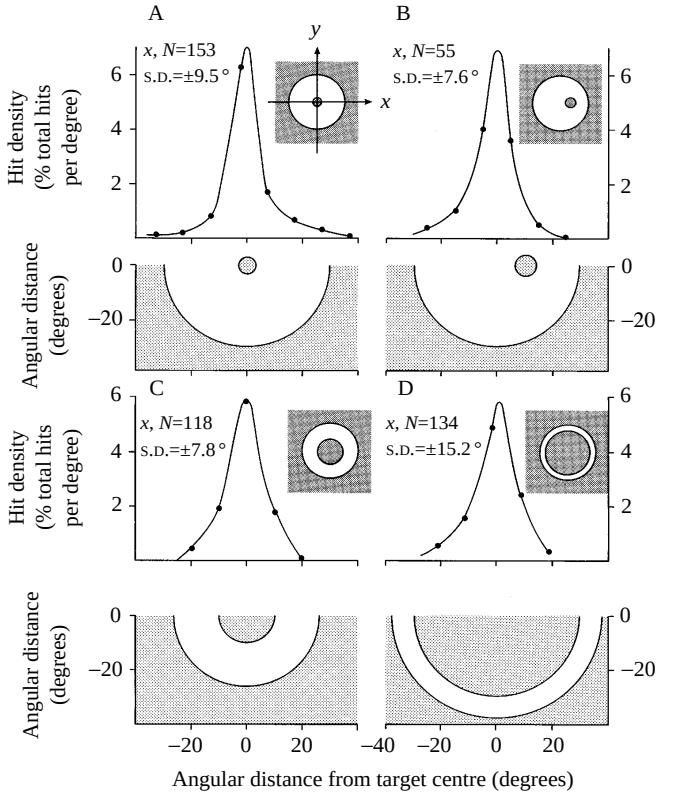

Fig. 7. Jump performance of *Empoasca vitis* against a disc of light containing a 7° diameter dark core located centrally (A) or eccentrically (B), or against rings of light (C,D). Only the distributions of the horizontal components of the take-off angles are given; hence, the two-dimensional distribution of trajectories could not be calculated. Other details as in Fig. 4.

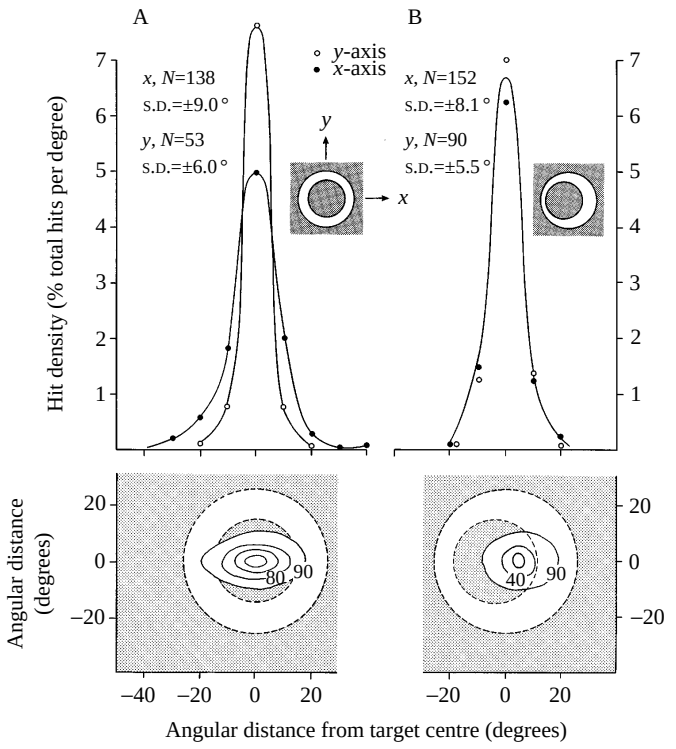

Fig. 8. Jump performance of *Empoasca* against a ring-shaped (A) or signet-ring-shaped (B) source of light. Other details as in Fig. 4.

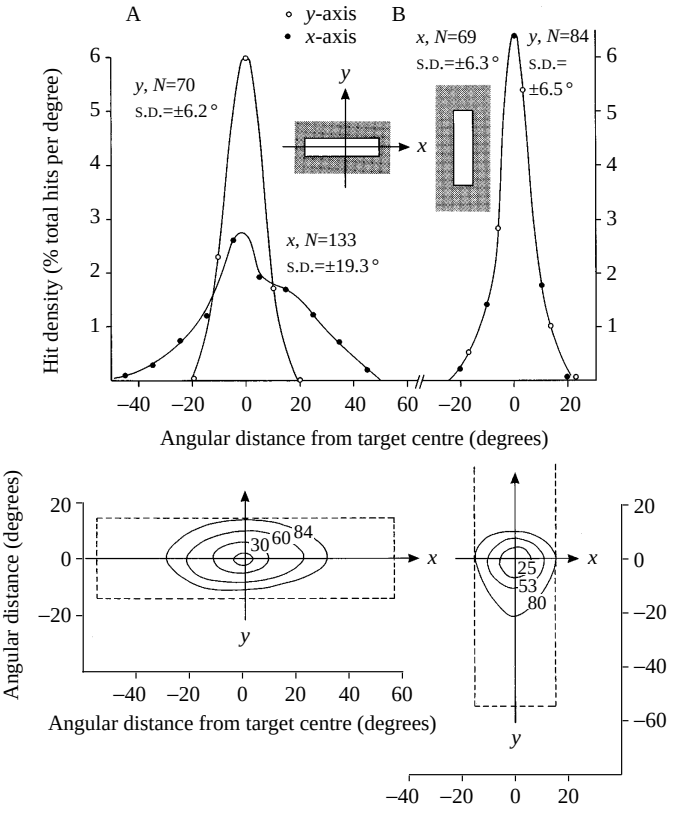

Fig. 9. Jump performance of *Empoasca vitis* against 32°×110° bar of light orientated horizontally (A) or vertically (B). Other details as in Fig. 4.

which in this case means that it is led towards the dark centre. The ability to locate the centroid of the light is considerably reduced in the case of a larger, thinner ring (external diameter 76°, internal diameter 60°) (Fig. 7D): the horizontal resolution is now little better than it was when targetting a 7° illuminated disc (Fig. 4).

Fig. 8 illustrates the accuracy with which changes in the location of the centroid of an illuminated shape can be located. The areas of the ring shape in Fig. 8A and the 'signet-ring' shape in Fig. 8B are equal, but the centroid of the latter area lies 3° to the right of that of the former. Note how, in each case, the point to which the jump trajectory was aimed coincided with the centroid.

A bar-shaped area of light (110°×32°) was targetted differently depending on whether it was orientated horizontally or vertically (Fig. 9). Whilst the vertical axial resolution was unchanged by the two orientations, the horizontal resolution improved threefold when targetting the vertical bar compared with the horizontal bar . This discrepancy mirrors the earlier finding using disc shapes that horizontal target resolution is sensitive to target width, but that vertical target resolution is insensitive to target height (or width). A plot of the individual S.D.*x*,S.D.*y* pairs obtained from all the experiments is given as a function of target width in Fig. 10. Although there are considerable gaps in the data, they confirm the relative invariance of S.D.*y* and suggest a peak in horizontal resolution (i.e. lowest values for S.D.*x*) for target widths of approximately 30–60°. The poorer horizontal resolution against a horizontal

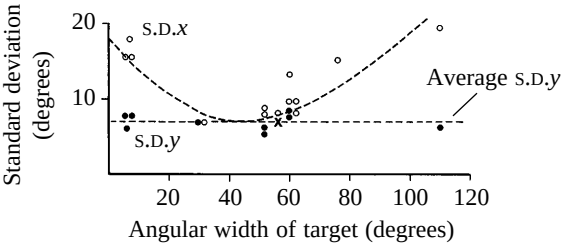

Fig. 10. Standard deviations of the horizontal (S.D.*x*, open circles) and vertical (S.D.*y*, filled circles) axial hit distributions as a function of angular width of the target. The lower dashed line indicates the mean S.D.*y* for all experiments (6.9°). The dashed curve is drawn through the S.D.*x* data.

bar of width 110° (Fig. 9A) compared with a vertical bar of width 32° (Fig. 9B) would be expected from Fig. 10. The mean S.D.*y* for all experiments was 6.9°. This appears also to be the value to which S.D.*x* converges in the region of optimal horizontal resolution.

The fall-off in the horizontal resolution of relatively large targets implies a loss in edge definition, or contrast perception, within the visual system as the boundaries of the image encroach upon the lateral visual field. To test this possibility, the insects were presented with double, vertically orientated bars, whose separation on the horizontal axis varied from zero

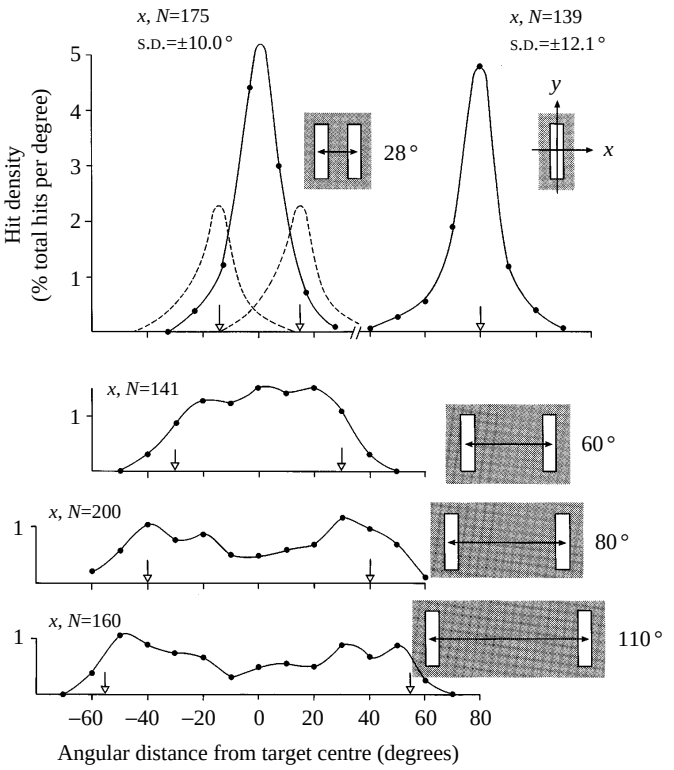

Fig. 11. Jump performance of *Empoasca vitis* against a double bar of light orientated vertically and at different bar separations. Open arrows represent the position on the *x*-axis of the centre of each bar. The dashed lines in the top left-hand graph show the expected distribution of take-off angles along the horizontal axis if the bars were targetted independently. Other details as in Fig. 4.

(i.e. a single bar) to 110° (Fig. 11). At a horizontal separation of 28°, the insects targetted the centre of the dark area between the bars (the centroid of the bar doublet) with at least the same accuracy as they targetted the centre of a single bar. At separations of 60° and above, however, there was a progressive tendency to target either one bar or the other. This was also visibly reflected in the behaviour of individual insects which, when confronted with the target, would often align the body axis first with one of the bars, then the other, as though undecided before making the jump.

Discussion

Kinematics

The fact that the take-off velocities of jumping homopterans are comparable to those of flea-beetles (Table 1) argues in favour of a similar reliance on a spring mechanism. Flea-beetles achieve high take-off accelerations and velocities using energy stored in a metafemoral spring (Furth *et al.* 1983). The structural basis of a catapult mechanism in jumping Homoptera has been described in the fulgorid *Pyrilla perpusilla* (Sander, 1956), although in this case the primary extensor muscles reside not inside the leg, but inside the thorax, and operate on the coxo-trochanteric joint. The latter joint is not used during walking but is reserved exclusively for springing, and synchronised extension of the legs is ensured by the presence of interlocking teeth on the medial surfaces of the closely applied metatrochanters.

Ballistic jumping overcomes the limitations of real-time muscular contraction in attempting to achieve high take-off accelerations, but at the same time it excludes any possibility of matching take-off velocity to range. In contrast, explosive jumpers, such as flea-beetles and leaf-hoppers, probably have little need for the relatively sophisticated method of distance perception and range-setting shown by locusts, grasshoppers and crickets (Wallace, 1957; Collett, 1978; Eriksson, 1980; Sobel, 1990; Goulet *et al.* 1981). One advantage of a high-velocity trajectory in ballistic jumpers is that it automatically preserves accuracy over distance (Brackenbury and Wang, 1995). Whilst this can be claimed for flea-beetles, it is not true in the case of *Empoasca vitis*: tthe rapid opening of the wings after take-off results in a trajectory which falls away rapidly under the force of gravity from the initial 'line of sight' prescribed by the eye. As explained in the Materials and methods section, once the wings are open, and the ballistic phase of the jump gives way to propulsion by the wings, the initial targetting accuracy rapidly deteriorates.

At the point of take-off, the body of most small leaping insects, including winged insects that take off before the wings are opened, experiences a pitching moment which leads to spinning, at rates as high as 187 Hz in the flea-beetle *Psylliodes affinis* (Table 1) and 480 Hz in the springtail *Sminthurus viridis* (Christian, 1979). Flea-beetles can abolish spin in mid-jump, by suddenly opening the wings. The very low rotation rates observed in Homoptera at the start of jumping (Table 1) appear to be exceptional since these insects also take off in a 'wingless' mode. Even before the wings of a leaf-hopper open, they exert a stabilising effect on the body because they extend well beyond the tip of the abdomen and provide a lifting surface posterior to the centre of gravity which counters pitching in the same way as the tail-fins of an aircraft. By the time the wings have fully opened, annulling pitching instability, the body has rotated through only a quarter of a cycle or less. Suppression of spin does not necessarily confer any benefits in terms of jump accuracy, but it does allow for the smoothest transition from jumping to flight and also, as in the case of the flea-beetle *Aphthona atrocaerulea*, maximises the probability of a feet-first landing in the event of a target being intercepted.

Targetting accuracy

The attraction of *Empoasca vitis* to the targets used in the present experiments is probably best described as a phototaxis, although one characterized by a very high degree of accuracy. The flickering nature of the light might have produced signal modulations at stationary retinal points, mimicking the effects of movement at the high-contrast boundaries and thereby adding to the attractiveness of the targets. Other insects, including mantids and flies, readily fixate flickering light sources (Pick, 1974; Lea and Mueller,

1977). Mantids, however, are capable of extracting much more information from the formal pattern and movement of images than is likely to be the case with *Empoasca vitis*. For example, when sorting visual stimuli into prey and non-prey categories, mantids take account of size, contrast and apparent speed of movement as well as configuration, i.e. the direction of movement in relation to orientation (Prete, 1993). None of the hit distributions produced by *Empoasca vitis* displayed any tendency beyond the relatively simple task of targetting the geometric centre of the two-dimensional light distribution. In particular, the high-contrast edges of the target image were not attractive. Movement cues may have been available to *Empoasca vitis*, including the flicker effect referred to above, and also any induced by the motion of the insect itself as it walked towards the target, but these did not seem to distract from the simpler task of locating the centroid of the illuminated image.

The differential responses to vertical and horizontal bars (Fig. 9) superficially suggests a discrimination on the basis of image orientation. Some insects, for example, display a preference for vertical as opposed to horizontal stripes (Schwind, 1978; Olberg, 1981; Collett, 1988; Collett and Paterson, 1991; Sobel, 1990). *Sphodromantis lineola* is particularly responsive to vertical bars moving downwards through the visual centre (Prete, 1993). Features of an image pattern such as bars or edges can be used by honeybees to discriminate orientation independently of cues obtained from motion (Srinivasan *et al.* 1993; Giger and Srinivasan, 1995) and specific orientation-tuned channels have been demonstrated in the dragonfly brain (O'Carroll, 1993). The visual system of *Empoasca vitis* may or may not be capable of such discriminations, but a much simpler explanation of the response shown to vertical and horizontal bars can be offered on the basis of biomechanical considerations, as will be discussed below.

Although the jumping behaviour of *Empoasca vitis* may be motivated by a simple phototaxis, the precision with which the centroid of the image is located suggests the involvement of a spatial sampling system that is nearly as accurate as, for example, the image-centring system of predatory insects. Rossel (1980) presented circular targets of 7°, 10° or 15° diameter in the lateral visual field of the mantid *Tenodera australasiae* and plotted the intersections of the direction of view of the fixation centre with the target, following saccadic head movements. It was clear from these experiments that *Tenodera australasiae* tries to locate the centre of such a target, and not its edges. The scatter of data about the target centre (S.D. 2–3°) was less than in the case of *Empoasca vitis* jumping (S.D. 7°), but *Tenodera australasiae* locates an image with the aid of a fovea, with interommatidial angles as low as 0.7°, and consequently a greater accuracy in such a task would be expected. The hunting carabid beetle *Notiophilus biguttatus* directs the frontal region of its eye towards prey with an accuracy similar to that characterising *Empoasca vitis* jumping (S.D. 5–10°, Fig. 5A; Bauer, 1981). The smallest directional correction made by *Notiophilus biguttatus* immediately before the final lunge was 2–3°, more in agreement with the size of the horizontal divergence angle between the frontal facets (2.2°).

Exactly how the image-centring process occurs in *Empoasca vitis* is beyond the scope of this paper, but its accuracy must ultimately depend on the space-sampling characteristics, and therefore the directionality, of the constituent photoreceptor units. The axial resolution of *Empoasca vitis* for optimal target sizes was 7°, expressed in terms of the standard deviation of the set of lines of sight prescribed around the centre of a given target. Assuming a normal distribution, a standard deviation of 7° means that 50% of all lines of sight, along either the *x*- or *y*-axis, would fall within a linear angle of ±5° of the centre. It is perhaps no coincidence that this value is almost exactly the same as that found during targetted leaping in the flea-beetle *Aphthona atrocaerulea* (6°, Brackenbury and Wang, 1995). As was stated in that study, a more precise gauge of the accuracy with which the task of *hitting* a target is achieved is based on the two-dimensional distribution of hits across the target area. In these terms, accuracy can be defined as the solid angle enclosing the central 50% of all recorded hits. In the case of *Aphthona atrocaerulea*, the resultant value was ±11°; from the lower part of Fig. 9B, the corresponding value measured in *Empoasca vitis* is approximately ±10°. Mathematically, the centroid of a uniformly illuminated regular or irregular shape can be defined as the unique point through which lines drawn between opposite points on the boundary (i.e. the pair of points formed by the intersection of a line passing through the centroid from the boundary of the shape) always (i) intersect the centroid at their own mid-point, and (ii) divide the area of the shape exactly into two. Whether the visual system of *Empoasca vitis* locates the centroid by areal summation, or by linear summation along radii scanned from paired points on the image boundary, is a matter of conjecture. Whatever system of optimisation is used, the possession of a central reference point, in the form of even a mildly expressed fovea, would clearly be advantageous.

The size-dependency of target resolution, at least of target resolution along the horizontal axis (Fig. 10), may genuinely reflect optical performance, but it may also be affected by changes in motivation. It is possible, for example, that the light from a 7° circular disc, which was more poorly targetted than the light from a 14° wide bar or a 60° wide disc, strikes only a very few facets, presents less total luminosity and overall contrast to the visual system, and is therefore less interesting. There is also some evidence that size-dependency may be influenced by target inclination, since the horizontal resolution against a 60° target was poor when the target was inclined at 45° compared with 28° (Fig. 6). One possible explanation is that the geometry of the target, as seen by the ommatidial array, changed with inclination. For instance, a circular disc mounted in the vertical plane would appear progressively more elliptical in shape with increased inclination. However, this is not likely to have been the case

since, in all the experiments with disc-shaped targets, the plane of the target was tilted towards the subject in proportion to the target inclination. If the insect were capable of aligning its body axis with the geometric centre of the target (and all the experimental evidence suggests that it is), the target shape would not change with inclination. Nevertheless, the results of Fig. 6 demonstrate the possibility of an influence of inclination on target resolution, and this subject would repay further examination in future studies. Optimal target size is also a feature of mantid behaviour, although the preference shown by this insect for indifferent stimuli subtending an angle of approximately 10 ° is also matched by its success in capturing similarly sized real items of prey (Maldonado and Rodriguez, 1972) and is of clear adaptive significance. A better key to understanding the poor targetting performance of *Empoasca vitis*, at least over the larger target size range, may be found in another aspect of mantis behaviour. A target image presented in the lateral visual field (47 ° from the visual centre) of *Sphodromantis lineola* failed to elicit saccadic head movements (Prete, 1993) and, similarly, *Tenodera australasiae* was not excited by targets placed 35 ° beyond the visual centre (Rossel, 1980). In mantids, images are more poorly defined in the peripheral field, because the interommatidial angles, and presumably the acceptance angles, are greater. Poor definition of the image boundary, leading to reduced spatial discrimination, could explain the failure of *Empoasca vitis* accurately to locate the centroid of larger images, and this interpretation is given some credance in the results shown in Fig. 11. At some point between 30 ° and 60 °, the visual system loses its ability to resolve the dark centre between an image doublet, and this is associated with a behavioural switch from trying to reconcile both images to concentrating on one alone. This may also reflect what happens when the insect is presented with a series of images of progressively increasing size: as the boundaries recede into the lateral visual field, there is a tendency for the insect to direct its gaze to the left or right (to increase image contrast at the boundary?), and this automatically produces a greater scatter of lines of sight about the centroid.

The final problem to be addressed in this study concerns the paradoxical invariance of the vertical axial target resolution with image size (Fig. 10). Outside the range of intermediate image sizes, where vertical and horizontal target resolution coincide quite closely, the visuomotor targetting performance along the vertical axis appears to exaggerate the true visual resolution capabilities of the eye. This is because visuomotor targetting, which is what is effectively measured in these experiments, is governed not only by visual but also by biomechanical constraints. The principal difference between the biomechanical constraints operating along the horizontal and vertical axes is that whereas the insect has total freedom to choose any angle within the equatorial plane at which to align its body, and therefore can prescribe any line of sight within this plane, its options within the vertical plane are limited to inclinations between 30 ° and 60 °. This results from limitations on the prothoracic and mesothoracic legs, which are responsible for moving the body up or down; the metathoracic limb is a non-participant in this ‘sight-setting’ process because the coxo-trochanteric joint constrains the leg to a single plane of movement. These biomechanical constraints automatically constrict visuomotor space in the vertical direction and therefore mask true target perception in that direction.

References

Bauer, T. (1977). The relevance of brightness to visual acuity, predation and activity of visually hunting ground-beetles. *Oecologia* **30**, 63–73.

Bauer, T. (1981). Prey capture and structure of the visual space of an insect that hunts by sight on the litter layer (*Notiophilus biguttatus* F., Carabidae, Coleoptera). *Behav. Ecol. Sociobiol.* **8**, 91–97.

Brackenbury, J. H. and Wang, R. (1995). Ballistics and targetting in flea-beetles (Alticinae). *J. exp. Biol.* **198**, 1931–1942.

Christian, von E. (1979). Der Sprung der Collembolen. *Zool. Jb. (allg. Zool.)* **83**, 457–490 (English summary).

Collett, T. S. (1978). Peering – a locust behaviour pattern for obtaining motion parallax. *J. exp. Biol.* **76**, 237–241.

Collett, T. S. (1988). How ladybirds approach nearby stalks: A study of visual selectivity and attention. *J. comp. Physiol.* A **163**, 355–363.

Collett, T. S. and Patterson, C. J. (1991). Relative motion parallax and target localisation in the locust *Schistocerca gregaria*. *J. comp. Physiol.* A **169**, 615–621.

Eriksson, S. (1980). Movement parallax and distance perception in the grasshopper (*Phalacridium vittatum*) *J. comp. Physiol.* **77**, 337–340.

Furth, D. G., Traub, W. and Harpaz, I. (1983). What makes *Blepharida* jump? A structural study of the metafemoral spring of a flea-beetle. *J. exp. Zool.* **227**, 43–47.

Giger, A. D. and Srinivasan, M. V. (1995). Pattern recognition in honey bees: eidetic imagery and orientation discrimination. *J. comp. Physiol.* A **176**, 791–795.

Goulet, M., Campan, R. and Lambin, M. (1981). The visual perception of relative distances in the wood-cricket *Nemobius sylvestris*. *Physiol. Ent.* **6**, 357–367.

Lea, J. Y. and Mueller, C. G. (1977). Saccadic head movements in mantids. *J. comp. Physiol.* **141**, 327–334.

Maldonado, H. and Rodriguez, E. (1972). Depth perception in the praying mantis. *Physiol. Behav*. **8**, 751–759.

O’Carroll, D. (1993). Feature-detecting neurons in dragonflies. *Nature* **362**, 541–543.

Olberg, R. M. (1981). Object-and-self-movement detectors in the ventral nerve cord of the dragonfly. *J. comp. Physiol*. **141**, 327–334.

Pick, B. (1974). Visual flicker induces orientation behaviour in the fly *Musca*. *Z. Naturforsch.* **29c**, 310–312.

Prete, F. R. (1990). Configural prey selection in the praying mantis, *Sphodromantis lineola* (Burr). *Brain Behav. Evol.* **36**, 300–306.

Prete, F. R. (1992). The discrimination of visual stimuli representing prey *versus* non-prey by the praying mantis, *Sphodromantis lineola* (Burr). *Brain Behav. Evol*. **39**, 285–288.

Prete, F. R. (1993). Stimulus configuration and location in the visual field affect appetitive responses by the praying mantis, *Sphodromantis lineola* (Burr). *Vis. Neurosci.* **10**, 997–1005.

PRETE, F. R. AND MAHAFFEY, R. J. (1993). Appetitive responses to computer-generated visual stimuli by the praying mantis, *Sphodromantis lineola* (Burr). *Vis. Neurosci.* **10**, 669–679.

ROSSEL, S. (1980). Foveal fixation and tracking in the praying mantis. *J. comp. Physiol.* **139**, 307–331.

ROSSEL, S. (1983). Binocular stereopsis in an insect. *Nature* **302**, 821–822.

SANDER, K. (1956). Bau und Funktion des Sprungapparates von *Pyrilla perpusilla* Walker (Homoptera-Fulgoridae). *Zool. Jb. (Anat)* **75**, 383–388.

SCHWIND, R. (1978). Visual system of *Notonecta glauca*: A neuron sensitive to movement in the binocular visual field. *J. comp. Physiol.* A **123**, 315–328.

SOBEL, E. C. (1990). The locust's use of motion parallax to measure distance. *J. comp. Physiol* **167**, 579–588.

SRINIVASAN, M. V., ZHANG, S. W. AND ROLFE, W. (1993). Is pattern vision in insects mediated by 'cortical' processing? *Nature* **362**, 539–540.

WALLACE, G. K. (1957). Visual scanning in the desert locust *Schistocerca gregaria*. *J. exp. Biol.* **36**, 512–525.